Ancestral amphibian *v2rs* are expressed in the main olfactory epithelium

Adnan S. Syed[a], Alfredo Sansone[b], Walter Nadler[c], Ivan Manzini[b,d], and Sigrun I. Korsching[a,1]

[a]Institute of Genetics, University of Cologne, 50674 Cologne, Germany; [b]Department of Neurophysiology and Cellular Biophysics, University of Göttingen, 37073 Göttingen, Germany; [c]Institute for Advanced Simulation, Juelich Supercomputing Centre, Forschungszentrum Juelich, 52425 Juelich, Germany; and [d]Center for Nanoscale Microscopy and Molecular Physiology of the Brain (CNMPB), 37073 Göttingen, Germany

Edited by John G. Hildebrand, University of Arizona, Tucson, AZ, and approved March 22, 2013 (received for review February 5, 2013)

Mammalian olfactory receptor families are segregated into different olfactory organs, with type 2 vomeronasal receptor (*v2r*) genes expressed in a basal layer of the vomeronasal epithelium. In contrast, teleost fish *v2r* genes are intermingled with all other olfactory receptor genes in a single sensory surface. We report here that, strikingly different from both lineages, the *v2r* gene family of the amphibian *Xenopus laevis* is expressed in the main olfactory as well as the vomeronasal epithelium. Interestingly, late diverging *v2r* genes are expressed exclusively in the vomeronasal epithelium, whereas "ancestral" *v2r* genes, including the single member of *v2r* family C, are restricted to the main olfactory epithelium. Moreover, within the main olfactory epithelium, *v2r* genes are expressed in a basal zone, partially overlapping, but clearly distinct from an apical zone of olfactory marker protein and odorant receptor-expressing cells. These zones are also apparent in the spatial distribution of odor responses, enabling a tentative assignment of odor responses to olfactory receptor gene families. Responses to alcohols, aldehydes, and ketones show an apical localization, consistent with being mediated by odorant receptors, whereas amino acid responses overlap extensively with the basal *v2r*-expressing zone. The unique bimodal *v2r* expression pattern in main and accessory olfactory system of amphibians presents an excellent opportunity to study the transition of *v2r* gene expression during evolution of higher vertebrates.

amino acid odorants | calcium imaging | TAAR | statistical test | spatial pattern

A hallmark of mammalian olfaction is the segregation of the sensory epithelium in several different olfactory organs, each with its own characteristic set of olfactory receptor gene expression, axonal connectivity, and function. However, in teleost fish, all olfactory receptor (OR) families share a common sensory surface. To what extent such differences influence the coding and discrimination abilities of the respective olfactory systems is unclear, and the evolutionary path toward such segregation is unknown. The analysis of amphibians, which are early diverging tetrapods compared with mammals, may shed light on this transition from shared sensory surface to segregated subsystems. Most amphibians already possess an accessory olfactory epithelium (1), the vomeronasal organ (VNO), which has been reported to express type 2 vomeronasal receptors (V2Rs), like the mammalian VNO (2), but in contrast to the latter is missing the type 1 vomeronasal receptors (V1Rs) that are instead expressed in the main olfactory epithelium (MOE) (3). These features suggest an intermediate expression pattern for olfactory receptor gene families in amphibians.

The MOE of both fish and mammalian species exhibits further subdivisions into distinct expression zones and domains (4, 5), and an initial analysis of the amphibian MOE has shown medial-to-lateral gradients of odor responses and corresponding gradients for expression of olfactory receptor genes (6). In that study, however, no candidate genes except one could be uncovered for responses to amino acids, one of the main odor groups for aquatic vertebrates. Because a fish *v2r* ortholog has been shown to respond to amino acids (7), we hypothesized that amphibian *v2r* genes could be candidates for amino acid detection. At first glance this may appear unlikely because all previously analyzed *v2r* genes are almost exclusively expressed in the VNO, with the exception of occasional rare cells in the larval and adult MOE (2). However, the amphibian *v2r* family is exceedingly large, with several hundred members in *Xenopus tropicalis* (8), and analysis of expression patterns has so far not been guided by phylogenetic considerations.

We have cloned several *v2r* genes not previously analyzed and representative of the three major phylogenetic subdivisions of the *v2r* family A as well as the single member of family C. We report here that family C is expressed exclusively in the MOE, together with earlier diverging members of family A, whereas later diverging family A genes are restricted to the VNO. Such a bimodal expression pattern in MOE and VNO has not been described in any species so far, and represents a noteworthy evolutionary intermediate between expression restricted to either the MOE or the VNO. Within the MOE, *Xenopus v2r* genes are expressed in at least two distinct basal expression zones, which overlap extensively with amino acid responses, but are clearly distinguishable from an apical expression domain containing receptors, transduction pathways, and odor responses associated with ciliated olfactory receptor neurons (ORNs) (6).

Results

RT-PCR Analysis Shows Segregation of the Amphibian V2R Family into MOE-Specific and VNO-Specific Genes. Though ~20 *Xenopus laevis v2r* genes have been cloned previously (2), their position in the phylogenetic tree has not been reported, and a systematic analysis of the *X. laevis v2r* family has not been possible due to the absence of a genome project. However, over 330 *v2r* genes have been identified in the genome of the closely related species *X. tropicalis*, the largest known *v2r* family (8). In the phylogenetic analysis using the same data set as Ji et al. (8), the presence of three major subgroups is apparent (Fig. 1), all of which belong to family A. We have selected five representative *v2r* genes (Fig. 1) from two of these groups, as well as Xl-*v2r-C*, the sole member of family C in *Xenopus*, and cloned their *X. laevis* counterparts by RT-PCR using primers derived from the *X. tropicalis* sequence. A gene representative of the third subgroup, x*v2r E-1*, had already been obtained previously (6). In all cases, we obtained *X. laevis* sequences that in BLAST searches (http://blast.ncbi.nlm.nih.gov/) showed the initially considered *X. tropicalis* gene as the closest ortholog. Though we have no way to measure how many *X. laevis v2r*s might cross-react with probes derived from our

Author contributions: A.S.S., I.M., and S.I.K. designed research; A.S.S., A.S., and S.I.K. performed research; W.N. contributed analytic tools; A.S.S., A.S., W.N., I.M., and S.I.K. analyzed data; and A.S.S., I.M., and S.I.K. wrote the paper.

The authors declare no conflict of interest.

This article is a PNAS Direct Submission.

Data deposition: The sequences reported in this paper have been deposited in the European Nucleotide Archive, www.ebi.ac.uk/ena/data/view/HF937211-HF937216 (accession nos. HF937211–HF937216).

[1]To whom correspondence should be addressed. E-mail: sigrun.korsching@uni-koeln.de.

This article contains supporting information online at www.pnas.org/lookup/suppl/doi:10.1073/pnas.1302088110/-/DCSupplemental.

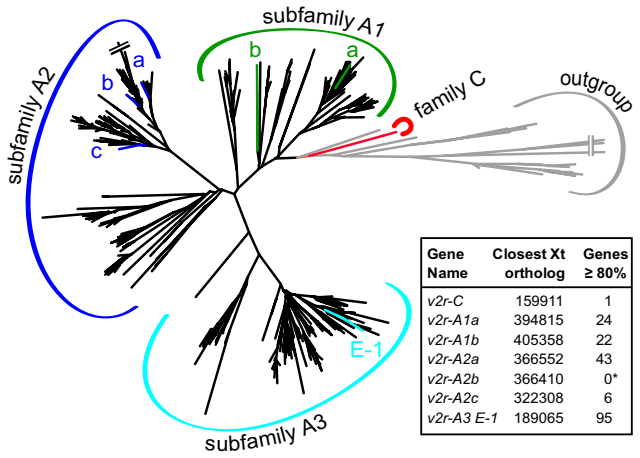

Gene Name	Closest Xt ortholog	Genes ≥ 80%
v2r-C	159911	1
v2r-A1a	394815	24
v2r-A1b	405358	22
v2r-A2a	366552	43
v2r-A2b	366410	0*
v2r-A2c	322308	6
v2r-A3 E-1	189065	95

Fig. 1. A phylogenetic tree of the *X. tropicalis* V2R repertoire was generated by a modified maximum-likelihood method (aLRT-ML). Colored branches refer to the nearest *X. tropicalis* orthologs of cloned *X. laevis* genes analyzed here. Note that amphibian *v2r-C* is a single gene, orthologous to the mammalian V2R-C family (8). (*Inset*) *X. laevis* genes analyzed here, as well as their closest orthologs in *X. tropicalis* and an estimate for the number of cross-reacting *v2r* genes (≥80% amino acid sequence identity to the *X. laevis* clones). *No close ortholog of *v2r-A2b* in *X. tropicalis*. Accession numbers have been deposited with the European Nucleotide Archive.

clones, we estimate from the sequence comparison with the *X. tropicalis v2r* repertoire that between 1 and 95 genes show ≥80% identity to our probes (Fig. 1). In total we expect our probes to sample the expression of at least half of the *X. laevis v2r* gene repertoire.

We performed RT-PCR of larval *X. laevis* tissues to analyze the tissue specificity of expression for the six representative *v2r* genes described above. As control for dissection accuracy of the closely neighboring VNO and MOE tissues, we examined the distribution of olfactory marker protein 2 (*omp2*), which in larval *X. laevis* is expressed exclusively in the MOE (9). An *omp2* band was absent from the VNO and only observed in the MOE (Fig. 2*A*), confirming the accuracy of the dissection. Three of the six genes were expressed in the VNO, with clear RT-PCR signals reproducibly found in the VNO, and signals absent from the MOE and other organs, such as brain and heart (Fig. 2*A*). Occasionally, weak or very weak bands were observed in other organs. This expression pattern is consistent with expectations from previous analysis for other *v2r* genes (2, 6).

For three other *v2r* genes, however, we found a highly unexpected result. We observed strong bands for the MOE, but none or occasionally very faint bands for the other tissues (Fig. 2*A*). Thus, *v2r* genes *v2r-C*, *v2r-A1a*, and *v2r-A1b* (and those genes cross-reacting with the corresponding probes) show a highly specific expression in the MOE, and are absent from the VNO and other organs. To the best of our knowledge, it is without precedent that major groups of a large olfactory receptor family are expressed in two different olfactory organs such as the VNO and the MOE. We therefore decided to analyze this highly unusual expression pattern at the cellular level by performing in situ hybridization.

Receptor Neurons in the MOE Express Early Diverging *v2r* Genes, but Vomeronasal Neurons Express Late Diverging *v2r* Genes. Expression of all *v2r* genes was examined by in situ hybridization of larval *X. laevis* tissue sections encompassing both VNO and MOE. Three of the genes, *v2r-A2a*, *v2r-A2b*, and *v2r-A2c*, are expressed exclusively in the VNO (Fig. 2), confirming results obtained by RT-PCR. These probes label sparse populations of cells, consistent with limited cross-reactivity to only a handful of other genes for each probe (Fig. 1). Of several hundred cells examined, a single labeled cell was detected in the MOE (Fig. 2), making the restriction of these genes to the VNO as stringent as that of the previously analyzed x*v2r E-1* (2, 6), which we include here for comparison (Fig. 2).

However, the three other *v2r* genes, *v2r-C*, *v2r-A1a*, and *v2r-A1b*, exhibit a strikingly different pattern of expression. We could not detect a single cell in the VNO for any of the three genes (Fig. 2). In contrast, all three genes show a strong expression in the MOE (Figs. 2 and 3), confirming our results obtained by RT-

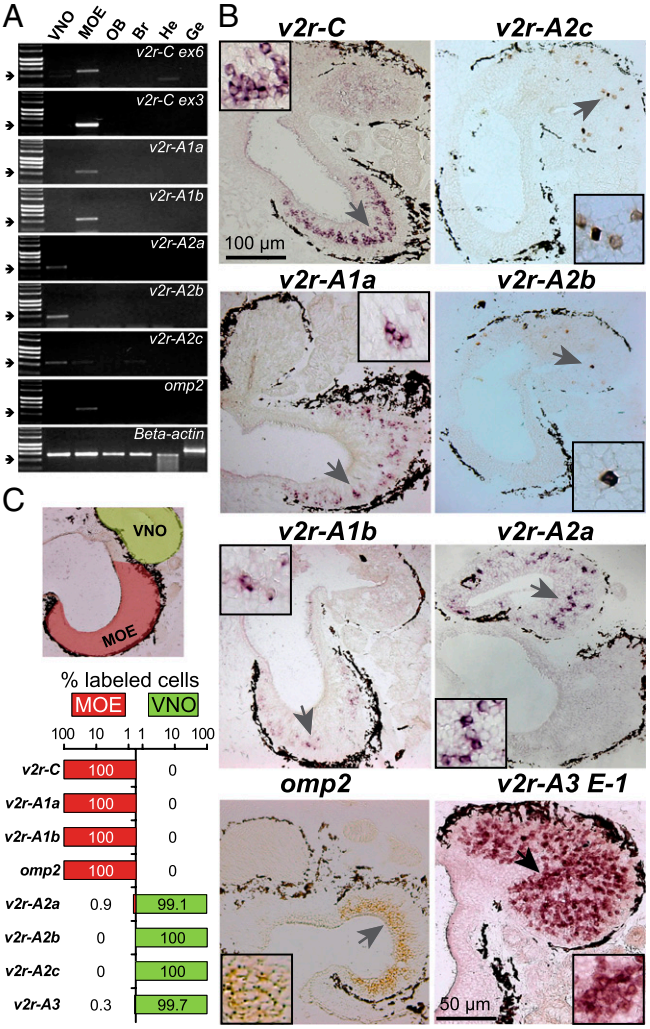

Fig. 2. Bimodal expression for the V2R family in MOE and VNO. (*A*) RT-PCR (40 cycles) was performed under stringent conditions; specificity does not change at higher cycle numbers. Lanes from left to right: VNO, MOE, olfactory bulb, brain, heart, and genomic DNA (in *Bottom* panel only). A β-actin intron-spanning probe was used as control for absence of genomic DNA contamination (*Bottom*). Arrows, 400-bp bands of molecular weight marker. (*B*) Cryosections of larval *X. laevis* were hybridized with antisense probes for seven *v2r* genes and *omp2* as depicted. Note the bimodal expression of *v2r* genes in either MOE (*Left*) or VNO (*Right*). Micrographs shown are from ventral horizontal sections of larval head tissue, which contain both VNO and MOE. VNO is above and/or to the right of the MOE, see also the colored overlay in *C*. Most probes cross-react with several to many other genes (Fig. 1), resulting in higher abundance of labeled cells. Scale bar for *v2r-C* valid for all panels except *v2r-A3 E1*. (*C*) Percentage of *v2r*-expressing cells in MOE (red bars) and VNO (green bars). Axis is shown on top; note the logarithmic scale. Over 100 to 350 cells (corresponding to 1–10 tissue sections) were analyzed per gene. For MOE-specific *v2r* genes, not a single cell was observed in the VNO, whereas very rare exceptions (2 of 677 cells) were seen for VNO-specific *v2r* genes.

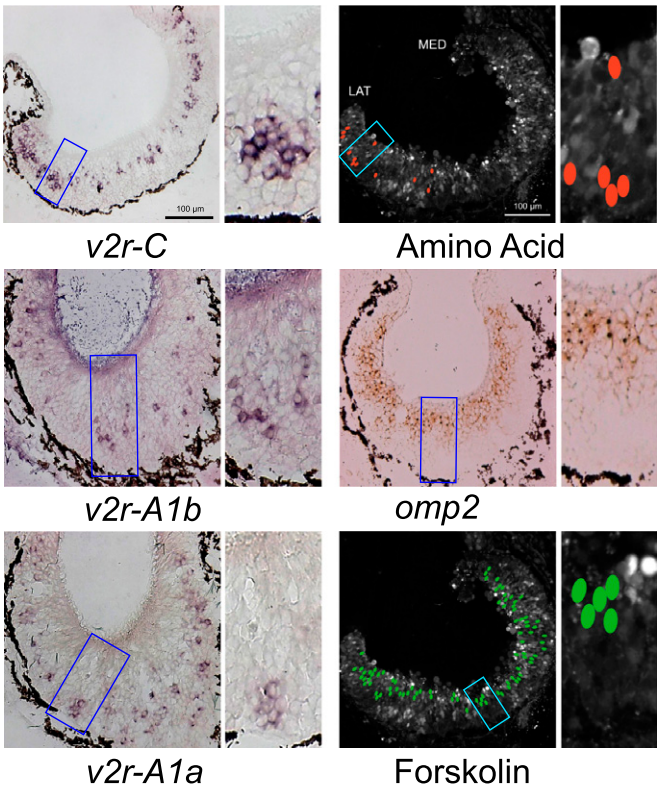

Fig. 3. A basal zone of the MOE is dedicated to *v2r* gene expression. In situ hybridization was performed for the three MOE-specific *v2r* genes and *omp2* using dorsal horizontal sections of larval head tissue. Enlargements from regions delineated by blue or cyan rectangles are shown to the right of each complete section. A ring of dark brown melanophores delineates the basal border of the epithelium; apical is toward the lumen. All *v2r* genes are enriched basally, whereas *omp2*-expressing cells are preferentially localized in an apical region. Forskolin- and amino acid-responsive cells were identified by calcium imaging (green and red ovals, respectively). Forskolin-responsive cells are apically enriched, very similar to *omp2*-expressing cells, whereas amino acid-responsive cells show a preferentially basal location.

PCR (Fig. 2*A*). Cell numbers for *v2r-A1a* and *v2r-A1b* are well above those expected for a single gene, but roughly consistent with our estimate of over 20 cross-reacting *v2r* genes for each (Fig. 1). The *v2r-C* probe is not expected to cross-react with other genes, but nevertheless labels an even larger population of cells (Fig. 2), similar to the broad expression of genes in the orthologous mammalian family (10). Thus, the MOE-specific *v2r* genes constitute a sizable group of the V2R repertoire and are expressed in a major neuronal population of the MOE.

For all seven *v2r* genes analyzed, a strong correlation is found between ancestrality in the phylogenetic tree and ancestrality in the mode of expression. All *v2r* genes with MOE-restricted expression reside in the earlier diverging subgroup A1 of family A or in family C (*v2r*-C), which is even less derived than the V2R-A1 subgroup (Fig. 1). In contrast, all *v2r* genes belonging to the later diverging subgroups A2 or A3 of family A (Figs. 1 and 2) are expressed exclusively in the VNO. In other words, more ancestral (earlier diverging) *v2r* genes of *X. laevis* are expressed in the more ancestral mode (in the MOE), like all the *v2r* genes of earlier diverging vertebrates, such as teleost fish. Complementarily, the more modern expression mode for *v2r* genes (expression in the VNO), is found for the more modern (later diverging) *v2r* genes among the amphibian *v2r* gene repertoire. This surprising correlation of phylogenetic position with expression mode is consistent with the notion that the transition from ancestral to derived mode of expression is a characteristic feature of later diverging *X. laevis v2r* genes.

MOE-Specific *v2r* Genes Are Expressed in a Basal Crescent. When examining results of in situ hybridization we noticed that the distribution of v2r-expressing cells within the MOE did not appear to be homogeneous. Both the apical and the basal region of the MOE are mostly devoid of labeled cells, and this feature of the distribution is constant over a wide range of dorsal/ventral locations, as seen by the comparison of more ventral (Fig. 2) with more dorsal sections (Fig. 3), although the latter contain up to 10-fold more cells. It is known that the basal layer contains progenitor cells and immature neurons (11), which could explain the dearth of *v2r*-expressing cells in this region. However, no such argument can be made for the near absence in apical regions, because nonneuronal supporting cells constitute just the outermost monolayer of cells (11, 12). Indeed, *omp2* expression is prominent in the apical region, and cells expressing trace amine-associated receptor 4a are also found in apical positions (Figs. 2 and 4). Albeit very distinct, V2R and OMP distributions are partially overlapping. Therefore, we performed quantitative analysis to examine the significance of the observed differences in the distributions.

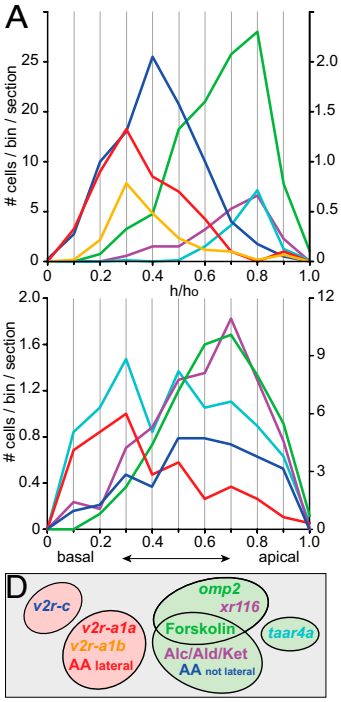

B

Gene / odor	peak (h/ho)	half-width	median (h/ho)	skewness
v2r-A1a	0.3	0.216	0.333	0.885
v2r-A1b	0.3	0.182	0.353	1.277
v2r-C	0.4	0.233	0.418	0.209
omp2	0.8	0.224	0.688	-0.527
xr116	0.8	0.201	0.710	-0.778
taar4a	0.8	0.099	0.774	-1.343
AA	0.3, 0.5	0.433	0.483	0.143
AA lateral	0.3	0.325	0.315	0.716
AA not lateral	0.6	0.300	0.590	-0.257
Alc/Ald/Ket	0.7	0.271	0.629	-0.460
Forskolin	0.7	0.280	0.652	-0.300

C

Gene/odor	gene/odor	p value
v2r-A1a	*v2r-A1b*	0.039
v2r-A1a	*v2r-C*	0.00002
v2r-A1b	*v2r-C*	0.0033
v2r-C	*omp2*	<0.00001
omp2	*xr116*	0.37
omp2	*taar4a*	<0.000001
Forskolin	Alc/Ald/Ket	0.0235
AA	Alc/Ald/Ket	0.00017
AA lateral	AA not lateral	0.000002
Forskolin	AA not lateral	0.041
AA lateral	*v2r-A1a*	0.132
AA lateral	*v2r-C*	0.00052
AA not lateral	*omp2*	0.001
Forskolin	*omp2*	0.0301
Alc/Ald/Ket	*omp2*	0.0016

Fig. 4. Basal-to-apical distributions were quantified for olfactory receptor genes and odor responses. (*A*) Receptor gene (*Upper*) and odor response (*Lower*) distributions are shown as histogram of relative height (0, most basal; 1, most apical position; bin size 0.1, bin center is shown). (*Upper*) *v2r-A1a* (red) and *v2r-A1b* (yellow) are centered basally; *v2r-C* (blue) encompasses both *v2r*-A1 receptors. *Omp2* (green), *xr116* (magenta, an *or* gene), and *taar4a* (cyan) are centered apically. Right *y* axis, *xr116*, and *taar4a*; left *y* axis, all others. (*Lower*) Forskolin (green), alcohol, aldehydes, and ketone responses (magenta) are centered apically, whereas amino acid responses (cyan) show a bimodal distribution (lateral, red; nonlateral, blue; Fig. S1). Right *y* axis, forskolin responses; left *y* axis, all others. (*B*) Characteristic parameters for the distributions shown in *A*. (*C*) Pairwise comparisons of different genes and/or odor responses were performed using the Kolmogorov–Smirnov test of the unbinned distributions. Distributions were considered significantly different for $P < 0.01$. (*D*) Venn diagram of differences between distributions. Entries within one circle share the same distribution; circles not overlapping correspond to different distributions. Note that the colors in *B*, *C*, and *D* correspond to those in *A* for receptors and odor responses, respectively.

Basal Expression Zone of MOE-Specific *v2r* Genes Is Significantly Different from an Apical Expression Zone for OMP2, OR, and Trace Amine-Associated Receptors. We used relative height (Fig. S1) as measure for the basal-to-apical dimension and evaluated 100–400 cells per gene. All three *v2r* genes showed a basal peak of expression, and their distributions appeared roughly similar to each other, as judged by peak position, median value, and skewness (Fig. 4 *A* and *B*). In contrast, the distribution of *omp2*-expressing cells was centered apically, had a much higher median value, and opposite sign skewness (Fig. 4 *A* and *B*). These features were shared by the distributions of two olfactory receptor genes, *xr116* (OR class I) and *taar4a*, albeit their cell density was only 1–2% of that of *omp2*.

In pairwise comparisons using the Kolmogorov–Smirnov test (13) we found that the apical-centered distribution of class I OR XR116 is highly similar to that of OMP2, whereas the apical-centered *taar4a* distribution is significantly different (Fig. 4*C*), suggesting further subdivisions within an apical expression zone defined by *omp2* expression.

Distributions of the basal-centered three MOE-specific *v2r* genes (*v2r-C*, *v2r-A1a*, and *v2r-A1b*) were significantly different from the apical-centered *omp2* (Fig. 4*C*; Table S1) and thus define a basal expression zone. Distributions for the two members of subgroup A1 are very similar to each other (Fig. 4*C*), but both are different from the V2R-C distribution (Fig. 4*C*; $P < 0.01$), which is slightly more broad, and whose median and peak values lie somewhat more apical (Fig. 4*B*). Thus, the expression zone defined by *v2r-C* may enclose *v2r-A1a* and *v2r-A1b* expression at its basal side, and other yet-to-be-identified *v2r* genes at its apical side. Together, the three MOE-specific *v2r* genes constitute a basal expression zone in the MOE, distinct from the apical expression zone of *omp2*-expressing neurons (Fig. 4 *A*–*D*).

A medial-to-lateral gradient perpendicular to the apical-to-basal gradient described here (Fig. 5) was identified in a previous study (6) for several genes and odor responses. Preferred positions in both dimensions do not appear to be correlated (apical and lateral preference for TAAR4a vs. apical and medial for XR116). To analyze a possible interdependence between preferred positions on both axes more rigorously, we compared for all genes height distributions for medial, intermediate, and lateral segments. We report that height distributions in all three segments are indistinguishable for each of the three *v2r* genes, as well as for *omp2*, *xr116*, and *taar4a* (Fig. S1; Table S2). Furthermore, all three *v2r* genes and *omp2* do not show enrichment or depletion along the medial-to-lateral axis (Table S3; Fig. 5), unlike *xr116* and *taar4a* (6). Taken together, these data are consistent with the hypothesis that preferred positions in each dimension are specified independently.

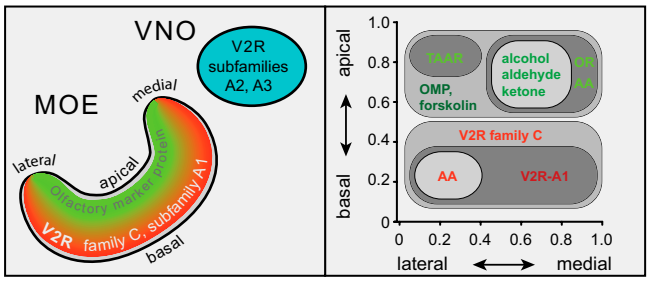

Fig. 5. Bimodal and zonal topology of *v2r* gene expression and odor responses. (*Left*) Complementary expression of two groups of *v2r* genes in MOE (*v2r-C* and two *v2r-A1* genes) and VNO (*v2r-A2* and *v2r-A3* genes). Within the MOE, gradients of expression frequency are observed. A basal zone (red) contains the *v2r* genes, whereas an apical zone (green) contains OMP2 as well as an odorant receptor; forskolin; and alcohol, aldehyde, and ketone responses (not depicted). (*Right*) A 2D schematic representation of the center region of each odor response and gene expression analyzed. Amino acid responses are heterogeneous, basal in the lateral segment, but apical in the intermediate and medial regions. In all, multiple subdivisions are observed, resulting in a highly complex pattern.

Amino Acid Responses Show a Bimodal (Apical and Basal) Distribution, Whereas Forskolin Responses Are Restricted to an Apical Zone. This independence of preferred positions in the two dimensions allows us to test the tentative assignment of receptor gene families to odor responses, which we derived from the correlations between receptor expression and odor responses in the medial-to-lateral dimension (6). We had concluded that ciliated receptor neurons may express class II *or* and some class I *or* genes and respond to alcohols, aldehydes, and ketones, and had found a single gene, *taar4a*, with an expression pattern correlating to amino acid responses. These two odor responses segregate nearly completely (6), thus defining the medial and lateral stream of odor processing, and were chosen here together with forskolin, an activator of adenylate cyclase (6), for analysis of basal-to-apical distribution.

Responses were measured as calcium signals using a previously established imaging method (14). Forskolin-responding cells were situated preferentially apically (Fig. 3), very similar to responses to alcohols, aldehydes, and ketones. Indeed, these two distributions did not differ significantly in the basal-to-apical dimension (Fig. 4*C*), suggesting that responses to these odors may be carried mostly by forskolin-responsive ORNs, i.e., ciliated neurons (15). Interestingly, responses to the mixture of alcohols, aldehydes, and ketones are more restricted than those to forskolin in the other, the medial-to-lateral, dimension (Fig. S1; Table S3), suggesting that the former may represent a spatially restricted subpopulation of the latter.

Unexpectedly, amino acid stimuli evoked responses in basal as well as apical cells, resulting in a broad and bimodal distribution (Fig. 4 *A* and *B*; Tables S1 and S2), significantly different from all other genes and odor responses (Fig. 4*C*; Tables S1 and S2). This finding might be explainable by a heterogeneous population of amino acid-responsive cells, because the sum over two different distributions would result in two peaks and increased half-width. To test this assumption, we examined the apical-to-basal distribution of amino acid responses separately for the three subregions (medial, intermediate, and lateral) defined previously (6). Lateral cells show a basal distribution, whereas nonlateral (intermediate and medial) cells exhibit a preferentially apical localization (Figs. 4 *A* and *B* and 5; Fig. S1), significantly different from the distribution of basal cells, but very similar to forskolin responses (Fig. 4*C*). Moreover, median values are distinctly different for the lateral and the nonlateral population, and in particular half-width for both is much smaller than for the total population (Fig. 4*B*). These data provide evidence for two distinct amino acid response systems of similar abundance (Fig. 4*A*; Table S3) (6), one centered basolaterally, the other one apical and nonlateral. In comparison, the apical-to-basal distributions of forskolin responses in medial, intermediate, and lateral segments are very similar in all quantitative parameters (Fig. S1; Table S2), consistent with cells in all three segments belonging to the same population.

Two *v2r*-A Genes Define Subregions in the V2R Expression Zone Similar to Those of Lateral Amino Acid-Responsive Cells. Amino acids constitute one of the main classes of odor stimuli for aquatic vertebrates (16). TAAR4a emerged as a candidate receptor in a previous study (6) due to the remarkable similarity of its medial-to-lateral distribution to that of amino acid-responsive cells. However, in the apical-to-basal dimension the correlation of TAAR4a expression with amino acid responses breaks down, because TAAR4a is found in the apical expression zone throughout medial, intermediate, and lateral segments, whereas amino acid responses are localized basally in the lateral zone and apically in the nonlateral segments (see above). These results directly exclude an involvement of TAAR4a in the basolateral amino acid response, and also make an involvement in the apical and nonlateral amino acid response unlikely, because the TAAR4a expression zone is

CELL BIOLOGY

not restricted in the medial-to-lateral dimension in contrast to the laterally depleted apical amino acid response. Because the spatial distribution of a receptor is not expected to be broader than that of an odor response based on that receptor, we conclude that TAAR4a does not seem to be involved in either the basal or the apical amino acid response.

For comparison, the distribution of forskolin responses is similar to that of *xr116*, a *class I or* gene, in the medial-to-lateral dimension (6) as well as the apical-to-basal dimension (Fig. 4). Here the analysis of height supports the hypothesis formed by analysis of the medial-to-lateral distributions.

We show in this study the expression of a major population of *v2r* genes in the MOE. The large size of this receptor repertoire and the response of a fish V2R homolog to amino acids (7) as well as the expression of *v2r* genes in fish microvillous receptor neurons, which do respond to amino acids (17), led us to hypothesize that amphibian V2Rs could be candidates for amino acid detection. Indeed the apical-to-basal distribution of amino acid responses in the lateral region (Fig. 4) is very similar to that of *v2r-A1a* and *v2r-A1b* gene expression (Fig. 4; Table S2). However, *v2r-A1a* and *v2r-A1b* show no lateral enrichment (Fig. S1 and Table S3) and are therefore unlikely to be involved in the basolateral amino acid response. Other members of the V2R-A1 subfamily would appear to be the best candidates for mediating *Xenopus* amino acid responses.

Discussion

The most striking property of *Xenopus v2r* gene expression is the segregation of the family in MOE-expressing and VNO-expressing members, with the segregation apparently occurring according to phylogenetic distance. Earlier-diverging (more ancestral) genes are expressed exclusively in the MOE and later-diverging (more modern) genes are restricted to the VNO. This segregated expression pattern might be rather ancestral in the lineage of tetrapods, because lungfish express the V2R-correlated G protein Go both in their MOE and their vomeronasal primordia (18). However, a salamander, a later-diverging amphibian species compared with *Xenopus*, shows already the mammalian-like VNO-specific V2R and associated marker gene expression (19). Thus, VNO-restricted expression may have arisen more than once in later-diverging tetrapods, possibly each time during the transition to a terrestrial lifestyle and reflecting the concomitant restricted access of nonvolatile odors to the VNO in these species.

The three v2r genes analyzed here, *v2r*-C, *v2r-A1a*, and *v2r-A1b*, represent a major population of *v2r*-expressing olfactory neurons and a sizable part of the total *Xenopus v2r* repertoire, due to cross-reactivity. Moreover, MOE-specific expression was found in a large percentage (50%) of the *v2r* genes analyzed here. This pattern of expression is very different from the ectopic or broad expression of sporadic mammalian *or* and *v1r* genes (20, 21) and diametrically opposite to the very rare cells occasionally seen for more modern *v2r* genes of subgroup A2 and A3 both in larval MOE [this study and results by Hagino-Yamagish et al. (2)] and adult middle cavity (2), a subdivision of the MOE arising during metamorphosis (22). In fact, the restriction of the more ancestral *v2r* genes to the MOE is even stricter than that of the more modern *v2r* genes to the VNO, because we did not find a single exception in over 400 counted cells.

Furthermore, we show in the present study that within the MOE of *X. laevis*, *v2r* genes are expressed in a basal zone. In a quantitative analysis of the *v2r* distribution, it becomes obvious that there are no sharp borders of this basal zone. Instead, toward the apical region, a gradual decrease in frequency of expression is observed. This distinct, albeit broad distribution, is very reminiscent of similar distributions observed in the olfactory epithelium of teleost fish (4) and for some mammalian OR receptor genes (5).

The basal expression zone is defined by expression of *v2r-C* and is subdivided by the expression of *v2r-A1* genes. Such subdivisions have been reported for the expression of *v2r* genes in the mammalian VNO (23). It is remarkable that this vertical arrangement of zones and subzones may have survived the migration of *v2r* expression from the MOE to the VNO during the evolution of tetrapods. The mammalian *v2r-C*-orthologous family is coexpressed with other *v2r* genes (10, 24), and the *v2r-C* localization described here is consistent with an analogous role of the *Xenopus* V2R-C.

Within the apical zone, the *omp2* distribution is indistinguishable from the forskolin distribution, and an individual *or* gene (*xr116*) exhibits a scaled-down version of the same distribution. In contrast, the *taar4a* distribution, albeit apical as well, is significantly different and much narrower; it is unclear whether this is related to the diminutive size of the *taar* gene family in *Xenopus* (25). Thus, the apical domain, as well as the basal domain, appears to have further subdivisions, resulting in a complex picture of spatial regulation of olfactory receptor gene expression.

Interestingly, the apical-to-basal distribution of lateral amino acid-responsive cells fits closely to the *v2r-A1a* distribution, whereas the apical-to-basal distribution of intermediate and medial regions resembles the *omp2* distribution. Thus, amino acid-responsive cells appear to form a heterogeneous population. Amino acid-responsive ORNs are laterally enriched, as are markers for microvillous receptor neurons (6), and so the simplest explanation for the observed distributions would be that the observed amino acid responses are the sum of a lateral population of microvillous, *V2R*-expressing ORNs combined with a nonlateral population of ciliated, *omp2*-expressing ORNs; this would parallel previous observations of ciliated ORNs responding to amino acids in some fish species (26).

Combining all spatial expression patterns obtained in this and a preceding analysis (6) leads us to hypothesize two dimensions of gene segregation: a medial-to-lateral dimension (6) and an apical-to-basal dimension transversing the epithelial layer (this study). The coordinates in these two dimensions appear to be specified independently, because many different combinations of preferred positions are observed (Fig. 5). In both dimensions, distributions are broadly overlapping, but nevertheless distinctly identifiable by parameters such as half-width, median, and skewness, as well as by statistical tests (13, 27).

In sum, we identified a unique expression pattern for the amphibian *v2r* family in both MOE and VNO and found a particular domain of the MOE dedicated to *v2r* expression. Further study is required to elucidate the molecular mechanisms underlying the ontogenesis of such restricted expression patterns, which could involve either directed migration or regiospecific determination of neuronal cell fate within the MOE. Foremost, it will be exciting to reveal the differences between VNO-residing V2Rs and those expressed in the MOE, in terms of function and of expression regulation. The *Xenopus* olfactory system appears uniquely suited to analyze such questions.

Materials and Methods

Phylogenetic Analysis. The complete set of *X. tropicalis v2r* sequences (8) was aligned using MAFFT, version 6, and E-INS-i strategy with default parameters (http://align.bmr.kyushu-u.ac.jp/mafft/online/server/). Phylogenetic trees were constructed using a modified maximum-likelihood method, aLRT-PhyML (28), as implemented on the Phylemon2 Web server (http://phylemon.bioinfo.cipf.es/index.html). For the visualization of the phylogenetic tree, Phylodendron was used (http://iubio.bio.indiana.edu/treeapp/treeprint-form.html).

Animal Handling. All procedures for animal handling were carried out according to the guidelines of the Göttingen University Committee for Ethics in Animal Experimentation. Larval *X. laevis*, stages 50–54, staged after ref. 29, were cooled to produce complete immobility and killed by transection of the brain at its transition to the spinal cord.

Cloning. Nonambiguous primers were designed based on published sequence information or homologous sequences in *X. tropicalis* (Table S4). Conserved regions among mouse, fish, and frog *v2r-C* sequences were used to guide the choice of primers for *v2r-C*. For genes from the *v2r-A1* and *v2r-A2* subfamilies,

regions conserved within their respective subfamilies were chosen. Annealing temperatures between 55 °C and 58 °C were used with genomic DNA as template. Resulting fragment lengths varied from 200 to 500 bp. All fragments were cloned into pGEM-T (Promega) and later confirmed by sequencing.

RT-PCR. Total RNA was extracted from *X. laevis* tissues using the innuPREP DNA/RNA Mini Kit (Analytik Jena) and Omniscript Reverse Transcriptase (Qiagen) for first-strand cDNA synthesis. PCR primer and PCR conditions were as stated above.

In Situ Hybridization. Digoxigenin-labeled (DIG; Roche Molecular Biochemicals) RNA probes for in situ hybridization were prepared from the cloned DNA by using the same forward primers and reverse primers with a T3 promoter site attached to their 5′ end. For in situ hybridization, tissue blocks containing MOE and VNO were cut horizontally, fixed in 4% formaldehyde solution for 2 h at room temperature, equilibrated in 30% saccharose, and embedded in Jung tissue-freezing medium (Leica). Cryostat sections of 10–12 μm (Leica CM1900) were dried at 55 °C and postfixed in 4% (wt/vol) paraformaldehyde for 10–15 min at room temperature. Hybridizations were performed overnight at 60 °C using standard protocols [50% (vol/vol) formamide]. Anti-DIG primary antibody coupled to alkaline phosphatase and NBT (4-nitro blue tetrazolium chloride), BCIP (5-bromo-4-chloro-3-indolyl-phosphate) (NBT-BCIP) (both from Roche Molecular Biochemicals) were used for signal detection.

Calcium Imaging. Odor responses were measured as changes of intracellular calcium concentrations of individual ORNs in Vibratome slices of the olfactory organs using Fluo-4/AM as calcium indicator dye, essentially as described (12). Odorant stimuli [an amino acid mixture and a mixture of alcohols, aldehydes, and ketones (6)], and forskolin, an activator of adenylate cyclase and therefore the cAMP signaling pathway, were applied by gravity feed and used at 100 μM final concentration per compound (50 μM for forskolin). Minimum interstimulus interval was 2 min to avoid adaptation, and reproducibility of ORN responses was verified by repeating the application of each stimulus at least twice.

Fluorescence images of the whole MOE were acquired at 1 Hz (excitation at 488 nm; emission above 505 nm) using a laser-scanning confocal microscope (LSM 510/Axiovert 100 M; Zeiss) and analyzed using custom programs written in MATLAB (MathWorks). Active ORNs were identified as regions of high cross-correlation between the fluorescence signals of neighboring pixels (30). The diameter of such regions was typically 6–10 μm, consistent with these signals emanating from the somata of individual ORNs (14). Optical section thickness was chosen to ensure that observed signals originated from single cells. Ten images before the onset of stimulus application were taken as control (F_0). A response was considered significant if the first two fluorescence values after stimulus arrival at the mucosa, F_1 and F_2, were larger than the maximum of the F_0 values, and if F_2 was larger than F_1 (12).

Analysis of Spatial Distribution. The position of cells was evaluated in two dimensions perpendicular to each other, medial-to-lateral and basal-to-apical. Position in the first dimension was determined according to ref. 6, and in the second dimension by measuring the relative height of the cell, defined as distance of the cell soma center from the basal border of the epithelium divided by total thickness of the epithelial layer at the position of the cell ($h_{rel} = h_{cell}/h_{layer}$; Fig. S1). Cell positions were measured using ImageJ (http://rsbweb.nih.gov/ij/) and/or manually on printouts.

Median, skewness, and half-width of the resulting spatial distributions were calculated from unbinned values using Open Office (version 3.2; www.openoffice.org/). Half-width of a height distribution was defined as difference between the values for the upper quartile and the lower quartile. The peak value was taken from the graphical representation of the histograms. To estimate whether two spatial distributions were significantly different, we performed Kolmogorov–Smirnov tests on the unbinned distributions as described in ref. 13. This test is particularly suitable for continuous distributions and makes no assumptions about the nature of the distributions investigated, which is essential because the skewness of the observed distributions showed that these are not Gaussian. Due to the sensitive nature of the test on large distributions ($n > 100$), we selected $P < 0.01$ as cutoff criterion for significant difference. Results of the Kolmogorov–Smirnov test were confirmed by permutation analysis (27) without exception.

ACKNOWLEDGMENTS. Mehmet Saltürk and Shahrzad Bozorgnia kindly provided clones for two *v2r*. We are grateful to Evangelia Tantalaki for DNA and RNA extraction and cDNA synthesis. This work was supported by Deutsche Forschungsgemeinschaft (DFG) Schwerpunktprogramm 1392 (to I.M. and S.I.K.), and Cluster of Excellence and DFG Research Center Nanoscale Microscopy and Molecular Physiology of the Brain (I.M.).

1. Eisthen HL (1992) Phylogeny of the vomeronasal system and of receptor cell types in the olfactory and vomeronasal epithelia of vertebrates. *Microsc Res Tech* 23(1):1–21.
2. Hagino-Yamagishi K, et al. (2004) Expression of vomeronasal receptor genes in *Xenopus laevis*. *J Comp Neurol* 472(2):246–256.
3. Date-Ito A, Ohara H, Ichikawa M, Mori Y, Hagino-Yamagishi K (2008) *Xenopus* V1R vomeronasal receptor family is expressed in the main olfactory system. *Chem Senses* 33(4):339–346.
4. Weth F, Nadler W, Korsching S (1996) Nested expression domains for odorant receptors in zebrafish olfactory epithelium. *Proc Natl Acad Sci USA* 93(23):13321–13326.
5. Mori K, Sakano H (2011) How is the olfactory map formed and interpreted in the mammalian brain? *Annu Rev Neurosci* 34:467–499.
6. Gliem S, et al. (2012) Bimodal processing of olfactory information in an amphibian nose: Odor responses segregate into a medial and a lateral stream. *Cell Mol Life Sci*, 10.1007/s00018-012-1226-8.
7. Luu P, Acher F, Bertrand HO, Fan J, Ngai J (2004) Molecular determinants of ligand selectivity in a vertebrate odorant receptor. *J Neurosci* 24(45):10128–10137.
8. Ji Y, Zhang Z, Hu Y (2009) The repertoire of G-protein-coupled receptors in *Xenopus tropicalis*. *BMC Genomics* 10:263.
9. Kashiwagi A, et al. (2006) Stable knock-down of vomeronasal receptor genes in transgenic *Xenopus* tadpoles. *Biochem Biophys Res Commun* 345(1):140–147.
10. Martini S, Silvotti L, Shirazi A, Ryba NJ, Tirindelli R (2001) Co-expression of putative pheromone receptors in the sensory neurons of the vomeronasal organ. *J Neurosci* 21(3):843–848.
11. Hassenklöver T, Schwartz P, Schild D, Manzini I (2009) Purinergic signaling regulates cell proliferation of olfactory epithelium progenitors. *Stem Cells* 27(8):2022–2031.
12. Hassenklöver T, et al. (2008) Nucleotide-induced Ca2+ signaling in sustentacular supporting cells of the olfactory epithelium. *Glia* 56(15):1614–1624.
13. Press WH, Teukolsky SA, Vetterling WT, Flannery BP (1992) *Numerical Recipes in C: The Art of Scientific Computing* (Cambridge Univ Press, Cambridge, UK), Vol 2.
14. Manzini I, Schild D (2004) Classes and narrowing selectivity of olfactory receptor neurons of *Xenopus laevis* tadpoles. *J Gen Physiol* 123(2):99–107.
15. Munger SD, Leinders-Zufall T, Zufall F (2009) Subsystem organization of the mammalian sense of smell. *Annu Rev Physiol* 71:115–140.
16. Caprio J, Byrd RP, Jr. (1984) Electrophysiological evidence for acidic, basic, and neutral amino acid olfactory receptor sites in the catfish. *J Gen Physiol* 84(3):403–422.
17. Koide T, et al. (2009) Olfactory neural circuitry for attraction to amino acids revealed by transposon-mediated gene trap approach in zebrafish. *Proc Natl Acad Sci USA* 106(24):9884–9889.
18. Nakamuta S, Nakamuta N, Taniguchi K, Taniguchi K (2012) Histological and ultrastructural characteristics of the primordial vomeronasal organ in lungfish. *Anat Rec (Hoboken)* 295(3):481–491.
19. Kiemnec-Tyburczy KM, Woodley SK, Watts RA, Arnold SJ, Houck LD (2012) Expression of vomeronasal receptors and related signaling molecules in the nasal cavity of a caudate amphibian (*Plethodon shermani*). *Chem Senses* 37(4):335–346.
20. Feldmesser E, et al. (2006) Widespread ectopic expression of olfactory receptor genes. *BMC Genomics* 7:121.
21. Fleischer J, Breer H, Strotmann J (2009) Mammalian olfactory receptors. *Front Cell Neurosci* 3:9.
22. Hansen A, Reiss JO, Gentry CL, Burd GD (1998) Ultrastructure of the olfactory organ in the clawed frog, *Xenopus laevis*, during larval development and metamorphosis. *J Comp Neurol* 398(2):273–288.
23. Herrada G, Dulac C (1997) A novel family of putative pheromone receptors in mammals with a topographically organized and sexually dimorphic distribution. *Cell* 90(4):763–773.
24. Ishii T, Mombaerts P (2011) Coordinated coexpression of two vomeronasal receptor V2R genes per neuron in the mouse. *Mol Cell Neurosci* 46(2):397–408.
25. Hussain A, Saraiva LR, Korsching SI (2009) Positive Darwinian selection and the birth of an olfactory receptor clade in teleosts. *Proc Natl Acad Sci USA* 106(11):4313–4318.
26. Hansen A, et al. (2003) Correlation between olfactory receptor cell type and function in the channel catfish. *J Neurosci* 23(28):9328–9339.
27. Manly BFJ (1997) *Randomization, Bootstrap and Monte Carlo Methods in Biology* (Chapman & Hall/CRC, London).
28. Anisimova M, Gascuel O (2006) Approximate likelihood-ratio test for branches: A fast, accurate, and powerful alternative. *Syst Biol* 55(4):539–552.
29. Nieuwkoop PD, Faber J (1994) *Normal Table of Xenopus laevis (Daudin)* (Garland, New York).
30. Junek S, Chen TW, Alevra M, Schild D (2009) Activity correlation imaging: Visualizing function and structure of neuronal populations. *Biophys J* 96(9):3801–3809.